Analysis of the Redox Reaction of an Archaebacterial Copper Protein, Halocyanin, by Electrochemistry and FTIR Difference Spectroscopy†

Martin Brischwein,‡ Birgit Scharf,§ Martin Engelhard,§ and Werner Mäntele*,‡

Institut für Biophysik und Strahlenbiologie, Universität Freiburg, Albertstrasse 23, 79104 Freiburg, Germany, and Max-Planck-Institut für Molekulare Physiologie, Rheinlanddamm 201, 44139 Dortmund, Germany

Received July 14, 1993; Revised Manuscript Received September 27, 1993®

ABSTRACT: Halocyanin is a recently discovered archaebacterial copper protein classified as "type I" small blue copper protein (Scharf, B., Ph.D. Thesis, University of Bochum, Germany). Its redox properties were investigated by a combination of protein electrochemical and spectroscopic techniques. Using electrochemical reactions in an ultrathin-layer electrochemical cell developed for UV/vis and IR spectroscopy, halocyanin could be quantitatively and reversibly oxidized and reduced. The titration of the absorption band at 600 nm can be perfectly described by a Nernst curve with $n = 1$ electron transferred; a quantitative fit yields a midpoint potential, E_m, of 183 mV (*vs* SHE) at a pH of 7.3. The midpoint potential falls constantly from +333 mV at pH 4 to +119 mV at pH 10, with three regions around pH 4.5, 6.5, and 8.5 where the pH dependence is ca. –60 mV/pH unit, indicating the uptake of a proton with the reduction. By analogy with other small type I copper proteins, the three pK values suggested by the pH dependency of E_m might be associated with three histidines which interact with the redox site. Electrochemically induced reduced-minus-oxidized Fourier transform infrared difference spectra in the 1800–1000 cm^{-1} range at neutral pH show a number of strong difference bands between ca. 1700 and 1600 cm^{-1} as well as smaller difference structures between 1600 and 1200 cm^{-1}. The maximum amplitude of the difference bands—only ca. 1% of the amide-I absorption at ca. 1639 cm^{-1}—indicates that only small protein rearrangements occur upon the redox transition. At the present stage, we tentatively assign a sharp difference structure at 1630(–)/1644(+) cm^{-1} to a special peptide C=O group serving as a fifth Cu ligand. The strong difference signal at 1704/1696 cm^{-1}, the two positive bands at 1663 and 1681 cm^{-1}, and the sharp negative feature at 1688 cm^{-1} are interpreted in terms of peptide C=O groups responding to conformational changes of the Cu-binding site. The reduced-minus-oxidized FTIR difference spectrum of halocyanin at pH 10 is similar overall to that at pH 7; only small frequency shifts and changes of band intensities are found for the bands attributed to peptide C=O groups, but changes of the band pattern are observed in the 1600–1700 cm^{-1} region. At pH 4, the strongest pH-dependent changes of the difference spectrum prevail, with two broad and intense bands at 1398 and 1557 cm^{-1} in the reduced form and a broad band at 1718 cm^{-1} in the oxidized form. These bands are assigned to the symmetric (1398 cm^{-1}) and antisymmetric (1557 cm^{-1}) COO^- vibration of the carboxylate and to the C=O vibration of the COOH group (1718 cm^{-1}) of an Asp or Glu side chain. The band structures are indicative of a proton uptake of an Asp or Glu side-chain group in halocyanin upon oxidation at low pH, which can be written as $H^+ \cdots Cu_{red} + R\text{–}COO^- \rightarrow Cu_{ox} + R\text{–}COOH$.

Small "type I" copper proteins play an important role in electron transport in plants and bacteria [for a review, see Rydén (1984)]. These proteins, which contain one copper atom in the typically 10 000–25 000 MW protein, exhibit a broad intense charge-transfer band at around 600 nm in the oxidized form and are thus termed "blue copper proteins". The X-ray structure analysis of *Pseudomonas aeruginosa* azurin (Adman et al., 1985) and of poplar plastocyanin (Colman et al., 1978) revealed a common motif of the Cu-binding site, which is formed by two nitrogens from histidines and two sulfurs from a cysteine and a methionine. In the case of stellacyanin, the methionine is exchanged by glutamine. As an additional fifth ligand in azurin, a peptide carbonyl is discussed (Rydén, 1984). This binding site structure is conserved in the copper-depleted apoprotein by a rigid protein structure. In the secondary structure, β-sheet domains dominate, and the variations among different small copper proteins mostly concern insertions and deletions in the loops, leaving the main topology unchanged.

Recently, a copper protein from the archaebacterium *Natronobacterium pharaonis* (Scharf, 1992; Scharf & Engelhard, 1993) was described. It was termed halocyanin according to the growth conditions of *N. pharaonis*, which are optimal at ca. 20% NaCl and a pH around 9. The intense blue color in the oxidized state, the content of 1 mol of Cu per polypeptide, and the redox activity have led to its preliminary classification within the group of "small blue" copper proteins. However, in contrast to, for example, plastocyanin or azurin, halocyanin appears to be a peripheral membrane protein and thus needs to be solubilized in detergent for purification (Scharf & Engelhard, 1993).

The role of halocyanin in the bioenergetic pathways of *N. pharaonis* is presently unclear and awaits the characterization of the membrane-bound soluble electron-transport components. Its structural analogy with other small blue copper proteins is extensive. In a separate paper, we will describe the analysis of the secondary structure of halocyanin by amide-I infrared spectroscopy (M. Brischwein, S. Grzybek, A. Barth,

† W.M. and M.E. acknowledge financial support from the Deutsche Forschungsgemeinschaft (Ma 1054/5-1; Ma 1054/9-1; EN 87/9-1). W.M. gratefully acknowledges a Heisenberg Fellowship from the DFG.

* Author for correspondence should be addressed.

‡ Universität Freiburg. Phone 49-761-203-5373. Fax 49-761-203-5016.

§ Max-Planck-Institut fur Molekulare Physiologie. Phone 49-231-1206-372. Fax 49-231-1206-389.

® Abstract published in *Advance ACS Abstracts*, November 15, 1993.

0006-2960/93/0432-13710$04.00/0

B. Scharf, M. Engelhard, and W. Mäntele, manuscript in preparation). The result confirms the classification of halocyanin as a small blue copper protein, with a predominant β-sheet content, as already inferred from UV-CD studies (Scharf & Engelhard, 1993), but with possibly a small fraction of α-helical form which might be associated with a membrane anchor.

In order to localize halocyanin in the electron-transfer chain of *N. pharaonis*, a detailed characterization of its redox properties, i.e., its midpoint potential (E_m), the number of transferred electrons (n), and a potential dependence of E_m on the pH (ΔE_m/pH), is essential. Furthermore, it is important to know about the intramolecular processes which accompany the redox reaction,and which could modify the surface properties of the molecule and control its docking to redox partners.

In previous investigations of small copper proteins, mostly chemical titrations were used to obtain E_m, n, and ΔE_m/pH, and only a few studies used electrochemical techniques like cyclic voltammetry or constant-potential electrolysis (Sykes, 1985; Armstrong et al., 1986; St Clair et al., 1992). Electrochemical titrations combined with spectroscopic measurements, compared to chemical titrations, provide the advantage of full reversibility and cyclic titration, no dilution of the solution with the oxidant or reductant, and a wider accessible potential range. We have recently reported the development of an ultrathin-layer spectroelectrochemical cell for the UV to IR range, which allows electrochemical titrations under spectroscopic control to be performed. This technique was applied to the study of the redox reaction of cytochrome *c* (Moss et al., 1990; Schlereth & Mäntele, 1993); of the pigments, quinones, and hemes in bacterial photosynthetic reaction centers (Mäntele et al., 1990; Moss et al., 1991; Fritz et al., 1992; Leonhard & Mäntele, 1993); and of hemoglobin and myoglobin (Schlereth & Mäntele, 1992). Using Fourier transform infrared (FTIR)[1] spectroscopy, reduced-minus-oxidized IR difference spectra of these redox proteins could be obtained. The spectral region of interest is the 1800–1000 cm^{-1} range, where contributions from Asp and Glu side-chain C=O groups (1760–1700 cm^{-1}) and peptide backbone C=O groups (1700–1620 cm^{-1}) as well as from several other amino acid side-chain residues are expected (Venyaminov & Kalnin, 1990a,b). The FTIR difference spectra reflect the readjustment of protein groups at or close to the redox sites to a new redox state, the conformational changes in the inner part of the molecule or at its surface upon undergoing a redox reaction, or the protolytic reactions which result from complex intraprotein electrostatics.

In a previous investigation of the well-known small copper protein plastocyanin (Moss et al., 1989), we have reported reduced-minus-oxidized FTIR difference spectra in this region. In the paper presented here, we report the electrochemical titration of halocyanin in an ultrathin-layer electrochemical cell, its midpoint potential, and its further redox properties, as well as the vibrational IR difference spectra, which provide evidence for distinct intraprotein reactions.

MATERIALS AND METHODS

Protein Preparation. Halocyanin was isolated from *N. pharaonis* as described by Scharf and Engelhard (1993) and stored at 4 °C in 50 mM phosphate buffer, pH 7.2, with 50 mM NaCl and 0.75% *n*-octyl D-glucopyranoside as a detergent. Redox activity was found unchanged under these conditions for several months. For IR spectroscopy, the protein was concentrated to approx. 1–2 mM using ultrafiltration cells (Centricon or Microcon cells from Amicon, Witten, Germany). Equilibration of halocyanin in D_2O was performed by repeatedly washing the sample in these ultrafiltration cells in an appropriate D_2O buffer, equilibrating for at least 24 h, and then reconcentrating to 1–2 mM.

The electrochemical cell used for the redox titrations was described previously (Moss et al., 1990) and used in a slightly modified version as described by Baymann et al. (1991). The surface of the gold mesh working electrode was chemically modified according to the procedure described by Hill et al. (1985) by adding a drop of a solution of pyridine-3-carboxaldehyde thiosemicarbazone (PATS 3). After 10 min, excess PATS 3 was removed with distilled water, and the mesh was dried. The PATS 3 molecules form a monomolecular layer on the gold electrode and prevent proteins from adsorbing and denaturing on it. The redox mediators used at a total concentration of 50 μM were essentially the same as described by Fritz et al. (1991).

For cell filling, a 5-μL drop of 1–3 mM halocyanin solution in 100 mM of the respective buffer (acetate buffer for pH 4–5, cacodylate buffer for pH 5–6, phosphate buffer for pH 6.6–8, borate buffer for pH 8.5–9.2, or borax–NaOH buffer for pH 10) containing the mediators and 250 mM KCl as electrolyte was placed at the center of the ca. 15-mm-diameter gold grid working electrode, which was layered on the bottom window of the cell [see Moss et al. (1990)]. With the second window mounted, the cell was placed between two metal plates of the cell holder, and pressure was applied uniformly on the cell to flatten the 5-μL drop to a full 20-mm diameter (corresponding to ca. 10-μm thickness). The buffer solution containing electrolyte was then injected through the side ports of the cell, and the working, reference, and counter electrodes were connected as described in Moss et al. (1990).

In addition to the electrochemical titrations in the thin-layer electrochemical cell for the visible and IR spectral region, which require high (millimolar) protein concentrations, redox titrations were performed in a flow cell built to our design with a 1-cm optical path length, which can be used with low (micromolar) protein concentrations for the visible range (Brischwein, 1992).

Spectroscopy. IR spectra were recorded on a modified Bruker IFS 25 FTIR spectrophotometer equipped with an MCT detector of selected detectivity at a resolution of 4 cm^{-1} and at a rate of 3 scans/s. UV/vis spectra were recorded using a home-built single-beam photometer integrated into the optics of the FTIR spectrophotometer (Mäntele, 1993). This arrangement allows the UV/vis and FTIR spectra of halocyanin to be recorded simultaneously in order to assess the redox state of the halocyanin in the course of the electrochemical reaction. The cell was thermostated at 6 °C. Electrochemical measurements were made with a potentiostat built to our design (Model Sevenich-Gimbel type II). The UV/vis and FTIR spectrophotometers and the potentiostat were controlled from data acquisition and treatment software (MSPEK) developed by S. Grzybek and D. A. Moss in our laboratory. All potentials quoted are *vs* SHE and are within ca. 5-mV precision.

RESULTS

Spectroscopy in the Vis/Near-IR Region. Figure 1 shows oxidized-minus-reduced difference spectra in the 450–900-

[1] Abbreviations: FTIR, Fourier transform infrared; OTTLE cell, optically transparent thin-layer electrochemical cell; SHE, standard hydrogen electrode; AU, absorbance units.

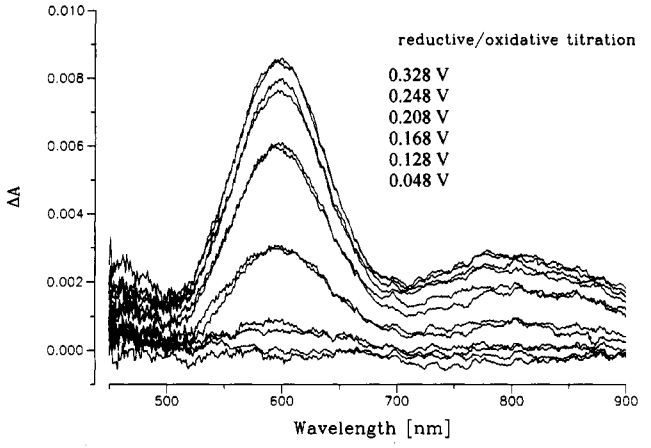

FIGURE 1: Oxidized-minus-reduced difference spectra of halocyanin selected from a reductive/oxidative titration in the spectroelectrochemical cell at pH 7.3 and 6 °C. All spectra were referenced to halocyanin equilibrated at 0.008 V (*vs* SHE). Spectra obtained for both senses of titration are plotted on top of one another. Conditions: 100 mM phosphate buffer, pH 7.3, with 250 mM KCl and a protein concentration of approx. 3 mM. Mediators were present as described in Materials and Methods.

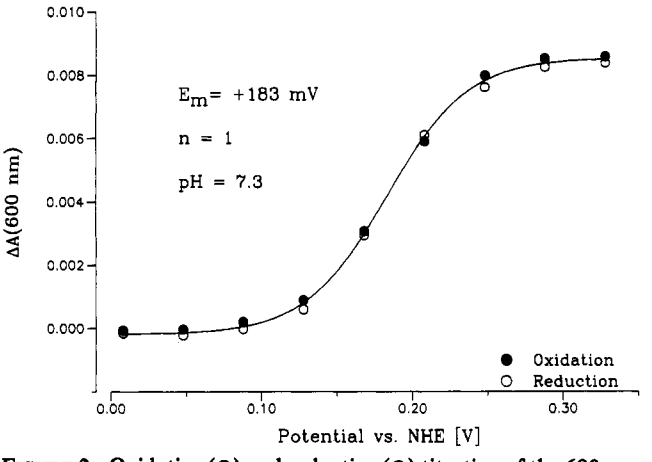

FIGURE 2: Oxidative (●) and reductive (○) titration of the 600-nm absorbance of halocyanin performed in the spectroelectrochemical cell. Data were taken from the spectra shown in part in Figure 1. The solid line represents a calculated Nernst function with $n = 1$ and E_m= +183 mV.

nm range of a halocyanin sample at pH 7.3 at the indicated potentials. Halocyanin in the thin-layer spectroelectrochemical cell was equilibrated for 1 min at a reducing potential (0.008 V *vs* SHE), and then a single-beam spectrum was recorded as a reference. The potential was then switched successively to more positive values; single-beam spectra were recorded at each potential after 1-min equilibration, and the absorbance spectrum was formed, taking the spectrum recorded at 0.008 V as reference. After oxidation of halocyanin at +0.328 V (top trace), the potential was lowered again in a reductive titration. The difference spectra of the oxidative and reductive titrations match perfectly, thus indicating complete equilibration of the protein with the electrode potential and full reversibility of the electrochemical reaction. These titrations could be repeated over many cycles without apparent decrease of reactivity or deviations for the amplitude of the 600-nm band.

Figure 2 shows the amplitude of the 600-nm band as a function of the applied potential taken from the titration shown in part in Figure 1. Open and closed circles represent the reductive and oxidative titrations, respectively. The titration of the 600-nm band can be closely approximated by assuming a single redox-active component. The solid line represents a

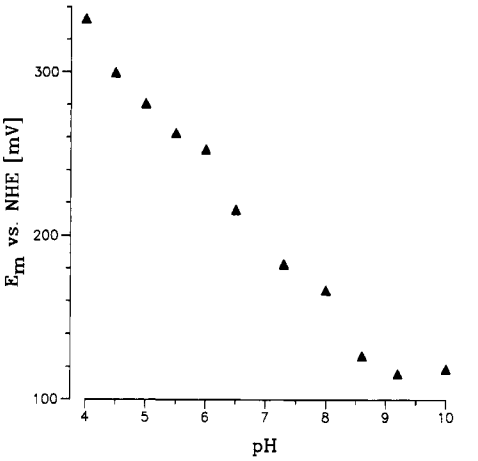

FIGURE 3: pH dependence of the redox midpoint potential. Data were obtained from spectroscopic titrations at the respective pH values, as in Figure 1, and approximated by $n = 1$ Nernst functions, as in Figure 2.

theoretical Nernst curve with $n = 1$ and E_m = +183 mV (*vs* SHE). Similar titration curves were obtained for the other charge-transfer bands at 460 and 790 nm (data not shown).

Figure 3 shows the variation of the midpoint potential over the pH range from 4 to 10. Lowering the pH to values below 4 leads to the slow disappearance of the characteristic blue color in the oxidized form, an effect which can be reversed upon raising the pH and may be ascribed to removal of the Cu^{2+} ion from the binding site and replacement by protons as proposed for azurins (Ainscough et al., 1987). Overall, the midpoint potential drops from +333 mV at pH 4 to +119 mV at pH 10 (*vs* SHE), with an average drop of −35 mV/pH. Three regions of stronger pH dependence can be discerned in Figure 3 around pH 4.5, 6.5, and 8.3, with a ΔE_m/pH of approx. −60 mV/pH. The midpoint potential may thus be governed by three protonable groups as indicated by this behavior.

Infrared Spectroscopy. The infrared absorbance spectrum of halocyanin equilibrated in H_2O shows an amide-I maximum at 1630 cm^{-1} with weak shoulders, in agreement with a predominantly β-sheet secondary structure. A detailed analysis of the amide-I band and a decomposition to different secondary structure elements will be given in a separate paper (M. Brischwein, S. Grzybek, A. Barth, B. Scharf, M. Engelhard, and W. Mäntele, manuscript in preparation).

In order to obtain oxidized-minus-reduced FTIR difference spectra, halocyanin was equilibrated at a reducing potential (0.008 V) for 5 min, followed by accumulation of 64 interferometer scans and Fourier transformation to a single-beam spectrum (I_1). After the potential was switched to +0.408 V and the sample was equilibrated for 5 min, the single-beam spectrum of oxidized halocyanin (I_2) was obtained from the same number of scans. The oxidized-minus-reduced difference spectra of halocyanin were obtained directly from the single-beam spectra of the sample equilibrated at the different potentials by calculating $A = \log(I_2/I_1)$. Several (up to 30) reduced-minus-oxidized spectra from successive electrochemical cycles were averaged to improve the signal-to-noise ratio. It should be noted, however, that no baseline subtractions, weighted subtractions of buffers, or data treatment procedures were performed.

Figure 4a shows the oxidized-minus-reduced FTIR difference spectrum of halocyanin at pH 7.0 in the 1800–1200 cm^{-1} range. Bands associated with the oxidized form thus appear positive, while negative bands are associated with the

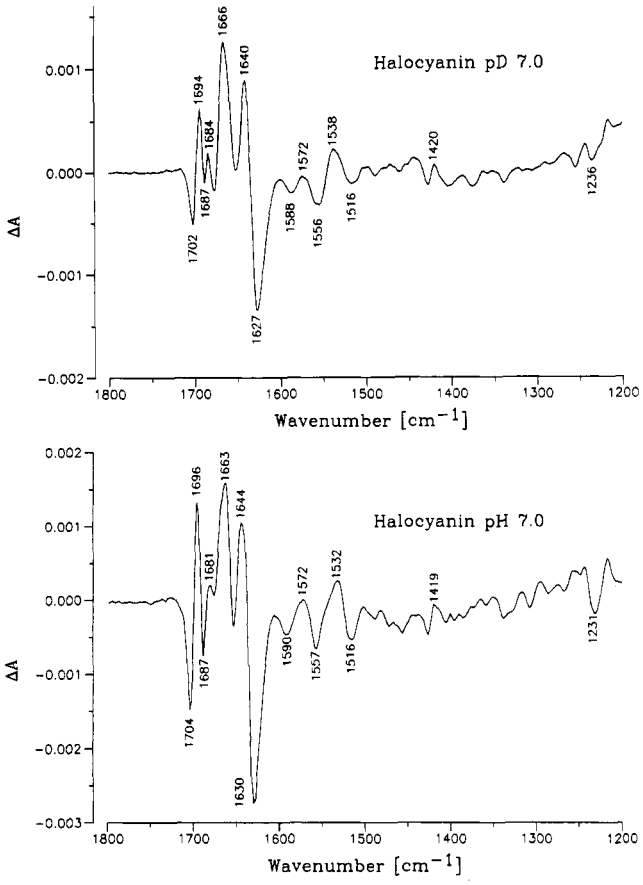

FIGURE 4: Oxidized-minus-reduced FTIR difference spectra of halocyanin in ^1H_2O (a, top) and ^2H_2O (b, bottom) at neutral pH/pD. The potential was switched from 0.008 to 0.408 V over several cycles, and 64 interferometer scans were accumulated for each redox state before Fourier transformation. Bands associated with the oxidized state point upward; those for the reduced state point downward. Conditions were as in Figure 1.

reduced form. The strongest difference bands correspond to approx. 2–3 × 10^{-3} absorbance units (AU) as compared to the amide-I absorbance at 1630 cm^{-1} of ca. 0.5 AU (data not shown; M. Brischwein, S. Grzybek, A. Barth, B. Scharf, M. Engelhard, and W. Mäntele, manuscript in preparation). The difference spectrum is dominated by strong bands in the 1600–1700 cm^{-1} range with a sharp differential band at 1704(–)/1696(+) cm^{-1}, a differential band at 1644(+)/1630(–) cm^{-1}, two positive bands at 1681 and 1663 cm^{-1}, and a sharp negative band at 1687 cm^{-1}. In addition, several weaker difference structures appear between 1600 and 1500 cm^{-1}.

Equilibration of halocyanin in ^2H_2O for 24 h leads to a reduction of the amide-II band intensity to <20% of its initial value (M. Brischwein and W. Mäntele, unpublished observations; M. Brischwein, S. Grzybek, A. Barth, B. Scharf, M. Engelhard, and W. Mäntele, manuscript in preparation), thus indicating significant exchange of the N-bound amide protons. The oxidized-minus-reduced FTIR difference spectrum shown in Figure 4b shows only minor shifts of bands and changes of band intensities compared to the spectrum in H_2O: The differential feature at the high-frequency side of the spectrum shifts by 2 cm^{-1} to lower wavenumbers, while the strongest differential band in the spectrum is found downshifted to 1640(+)/1627 cm^{-1}. The two bands at 1681 and 1663 cm^{-1} are both found upshifted by 3 cm^{-1}. As for relative band intensities, the amplitude of the highest frequency couple appears reduced, as is the case for the negative 1688 cm^{-1} peak and for the difference structures between 1600 and 1500 cm^{-1}.

The oxidized-minus-reduced FTIR difference spectra recorded in the pH range from 4 to 10 indicate pH-dependent vibrational frequencies and intensities. Although the main pattern of difference bands described in Figure 4a remained present throughout the whole pH range, smaller difference bands gradually appearing or disappearing with increasing pH indicate the titration of individual residues involved in local redox-induced conformational changes. The FTIR difference spectra at the extremes of the pH scale present the most prominent effects of pH. In order to exclude any interplay of the redox reaction with the buffer, which might result in a misinterpretation of buffer IR signals for signals of halocyanin, the spectra at pH 4 and 10 were repeated with halocyanin brought to the respective pH by addition of small aliquots of HCl or NaOH. In this case, the pH-dependent redox midpoint potential (*cf.* Figure 3) served as an internal control to determine the pH of these samples.

Figure 5a shows the oxidized-minus-reduced FTIR difference spectrum of halocyanin (unbuffered) under alkaline conditions, verified as being close to pH 10 by determination of the redox midpoint potential. We would like to emphasize that this difference spectrum is virtually identical to the one obtained in borate buffer at pH 10 (data not shown), except for a better signal-to-noise ratio, which is achieved by the higher protein concentration for the unbuffered sample. The main difference structures already observed at pH 7 (Figure 4a) are conserved at high pH, except for slight shifts of the strongest bands to 1628 and 1641 cm^{-1}. Further minor shifts are observed for the positive bands at 1681 cm^{-1} (to 1682 cm^{-1}) and at 1663 cm^{-1} (to 1661 cm^{-1}). The difference bands between 1600 and 1500 cm^{-1} exhibit considerably reduced intensity at high pH; in addition, changes of the band pattern are observed: Instead of the three negative bands at 1590, 1557, and 1516 cm^{-1} and the two positive bands at 1572 and 1532 cm^{-1} seen at neutral pH, three negative peaks at 1584, 1558, and 1535 cm^{-1} and two positive peaks at 1546 and 1525 cm^{-1} appear under alkaline conditions.

The oxidized-minus-reduced FTIR difference spectrum of halocyanin under acidic conditions (verified as pH 4 according to the midpoint potential) is shown in Figure 5b. As for the alkaline conditions shown in Figure 5a, the spectrum fully agrees with one obtained with halocyanin buffered at pH 4. The difference spectrum under acidic conditions shows a number of drastic changes with respect to that under neutral conditions. While the main differential features in the 1600–1700 cm^{-1} range are conserved, a broad positive band overlaps between ca. 1750 and ca. 1670 cm^{-1}. In addition, two negative bands of comparable width and intensity are observed, centered at 1570 and 1400 cm^{-1}. The structure in the negative band around 1570 cm^{-1} may result from the overlap of the negative bands at 1557 and 1590 cm^{-1}, which can be seen in the spectrum at neutral pH.

The main changes in the redox-induced FTIR difference spectrum between neutral pH and acidic conditions are more evident if a difference spectrum obtained at pH 6 is subtracted from that in Figure 5b. In the double-difference spectrum shown in Figure 5c, the sharp difference structures cancel almost completely, leaving the broad positive band at approx. 1700 cm^{-1} and the two negative bands at approx. 1400 and 1570 cm^{-1}.

DISCUSSION

UV/Vis Spectroscopy and Redox Properties. Small type I copper proteins exhibit an intense blue color in the oxidized state [Cu(II)], which arises from a charge-transfer band

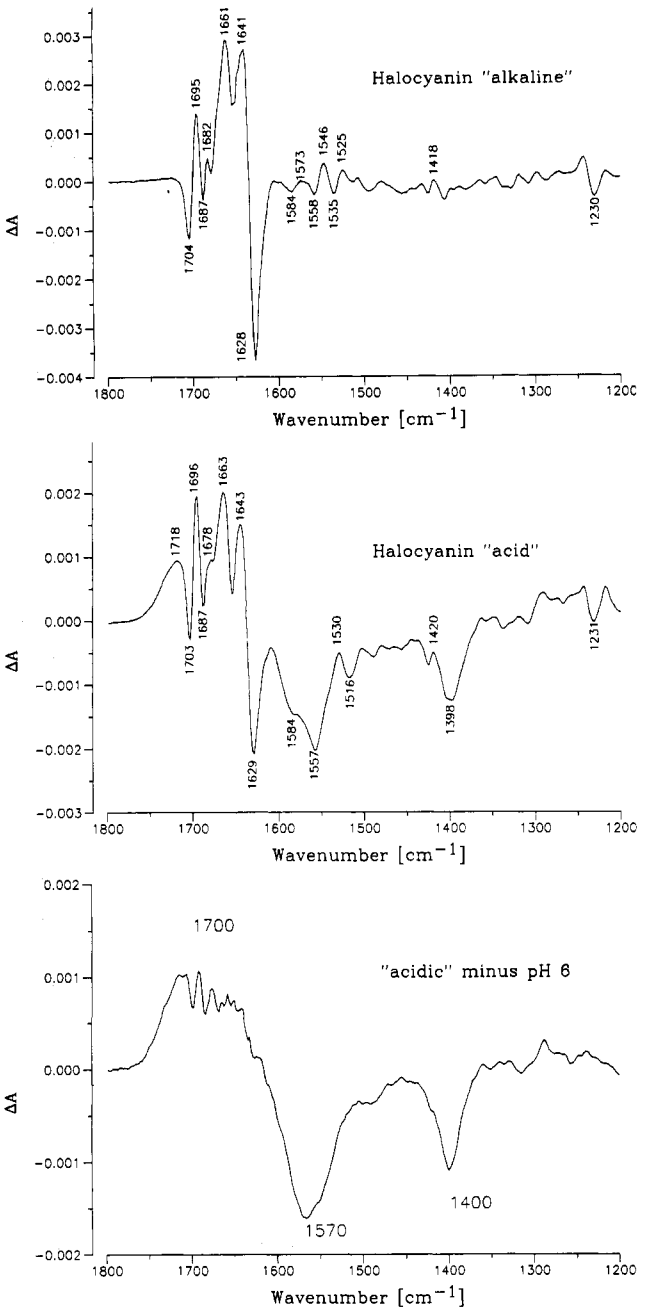

FIGURE 5: (a, top, and b, middle) Oxidized-minus-reduced FTIR difference spectra of halocyanin under alkaline (a) and acidic conditions (b). Four microliters of a concentrated halocyanin solution (approx. 5 mM) was mixed with 1 μL of a 0.3 M HCl or NaOH solution, respectively. The pH values were verified as being close to 4 (a) and close to 10 (b) by comparison with those obtained in buffers of pH 4 or 10 and by comparison of the redox midpoint potential determined for these samples with those shown in Figure 3. (c, bottom) Result of subtraction of a redox-induced difference spectrum at pH 6 from the difference spectrum at acidic conditions shown in Figure 5b.

(ligand····copper) located near 600 nm. The variation of the absorbance maxima from around 620 to 590 nm is thought to arise from differences in the hydrogen bonding of the ligand, which can stabilize the charge on the cysteine sulfur and reduce electron density at the copper. In addition, the different lengths of the Cu–ligand bonds might tune the electronic state. Table I summarizes some spectroscopic and redox properties of small blue copper proteins.

The intense blue color, the typical maximum of the charge-transfer band at 600 nm, and an extinction coefficient around 4000 L $mol^{-1}cm^{-1}$ (Scharf & Engelhard, 1993) place halocyanin well within the class of small blue copper proteins, with properties close to, for example, plastocyanin (λ_{max} = 597 nm, ϵ = 4500 L mol^{-1} cm^{-1}) (Rydén, 1984). The spectrum of oxidized halocyanin shows two side bands at 790 and at 460 nm, quite analogous to other type I copper proteins. Although no details on the structure of the copper-binding site are known to date, these charge-transfer bands and the content of 1 mol of Cu per polypeptide (Scharf & Engelhard, 1993) as well as conserved Cys, His, and Met in the amino acid sequence (Scharf & Engelhard, 1993) suggest strong analogies to the known Cu binding site structures.

Table I: Properties of Small Type 1 Blue Copper Proteins[a]

	MW	λ_{max} (nm)	E_m (*vs* NHE)	pH
azurin (*Pseudomonas aeruginosa*)	14 600	625	330	
azurin (*Alcaligenes faecalis*)	14 000	620	275	
auracyanin (*Chloroflexus aurantiacus*)	12 800	596	240	
amicyanin (from methylotrophic bacteria)	11 700	598	260	
plastocyanin (from poplar)	10 500	597	370	
umecyanin (from horseradish roots)	14 600	610	283	
plantacyanin (from cucumber seedlings)	10 100	597	317	
halocyanin (*Natronobacterium pharaonis*)	15 500	600	183	7.3

[a] Data from Ryden (1984), Adman (1985), and Sykes (1985, 1991).

Halocyanin reacts rapidly at the surface-modified gold grid electrode, either with PATS-3 (*cf.* Material and Methods) or with 2-mercaptoethylamine as electrode modifier. Kinetic traces of A_{600} recorded after a potential step (0 to +0.4 V) indicate formation of the oxidized species within <30 s in the presence of mediators or within 1–5 min without mediators (data not shown). This suggests that the electron transfer at the electrode is not the rate-limiting step, but rather that the equilibration time is dominated by the geometry of the cell (i.e., diffusion of the protein to the electrode). The current *vs* time traces (data not shown) and the identical difference spectra obtained in a reductive and an oxidative titration (*cf.* Figure 1) demonstrate quantitative and reversible electrode reactions.

Application of intermediate potentials led to titration of the charge-transfer bands; a plot of the amplitude of the 600-nm band *vs* the applied potential shows a Nernst behavior and can be fitted by a single one-electron transition. The midpoint potential determined for pH 6, +249 mV, is very close to that of *Alcaligenes faecalis* azurin (+276 mV) or auracyanin (+240 mV).

Previous titrations of other type I copper proteins revealed a dependence of the midpoint potential on pH (Sykes, 1991; St. Clair et al., 1992). The titration of halocyanin samples at pH values from 4 to 10 reveals an average drop of –35 mV/pH, considerably steeper than that of azurin. The data points in Figure 3 show three regions of stronger pH dependency, with a slope of –60 mV/pH, at pH values of approximately 4.5, 6.5, and 8.3. This suggests the involvement of three independently titrating residues which control the redox potential; however, a more complex model with interacting residues, leading to different slopes and p*K* values determined by the interaction energies, cannot be excluded at present.

For azurins, an influence of residues His 35, His 83, and His 32 (the latter only present in *Alcaligenes* azurin) on the redox midpoint potential was discussed (Sykes, 1991; St Clair et al., 1992). None of these His residues are involved in binding of the copper, and their distances are 8, 15, and 19 Å, respectively. These His residues were shown by ^{1}H-NMR to titrate independently with pK_s values between 4.8 and 7.6, with their pK_s values dependent on the redox state of the

copper. In return, the redox midpoint potential is a function of the pH value, in that protonation of these residues leads to a higher E_m. It might well be that a similar situation holds for halocyanin and that His residues control the redox midpoint potential, with three evident pK_s values. We shall return to this point in the discussion of the FTIR difference spectra at different pH values.

The determination of the pH dependence of the redox midpoint potential in the thin-layer cell and of the pH-dependent redox-induced FTIR difference spectra raises the problem of precise pH adjustment. This is a general problem for spectroscopic measurements at high (several millimolar) protein concentrations which are typical for IR investigations of proteins in aqueous (H_2O) solutions or suspensions where the path length is limited to <10 μm. The situation is even more difficult if thin semihydrated protein films are used as IR samples. A correct setting of the pH for such experiments implies that the buffering capacity of the buffer solution is significantly higher than that of the amino acid side chains. This may become a problem even with small proteins like halocyanin, where 30 of the 139 amino acids are Asp or Glu residues (S. Mattar, et al., unpublished observations). Given limited solubility of the buffers, or limited concentrations by reason of their IR absorbance, the effective pH may be shifted significantly from that of the initial buffer toward the isoelectric point of the protein [4.5 for halocyanin; see Engelhard and Scharf (1993)]. We have tried to cope with this problem by lowering the protein concentration as far as possible, keeping the buffer concentration as high as possible. An additional control of the correct buffering is provided by an independent determination of the redox midpoint potential for the protein at high dilution in an electrochemical flow cell with a 1-cm path length (Brischwein, 1992). The potentials determined in the thin-layer cell, with protein concentrations of 1–2 mM and buffer concentrations of 100 mM, and those determined in the flow cell, with protein concentrations of 5–10 μM and buffer concentrations of 100 mM, agreed within a few millivolts. We thus confidently use the conditions in the thin-layer cell for the determination of ΔE_m/pH and for the oxidized-minus-reduced vibrational difference spectra at different pH values. In addition, the dependence of the redox potential on pH can be used to determine the pH of an unbuffered halocyanin IR sample from its midpoint potential.

Infrared Spectroscopy. Redox proteins which only function as an electron carrier exhibit only small, but nevertheless distinct, structural changes associated with the redox transition. Evidence for this was provided, for example, for cytochrome *c* from the known X-ray structures (Takano & Dickerson, 1981), from amide-I second-derivative IR spectroscopy (Dong et al., 1992), or from redox-induced FTIR difference spectroscopy (Moss et al., 1990; Schlereth & Mäntele, 1993). In the case of type I copper proteins, small conformational changes in the Cu-binding site upon the redox transition were detected in the *Alcaligenes* azurin structure (Shephard et al., 1990). The distance from the axial ligands methionine and oxygen to the copper is supposed to increase by approx. 0.1 Å, together with other minimal rearrangements in the site. In contrast to this, EXAFS studies (Groenevald et al., 1986) suggest a decreasing Cu–S(Met) bond length upon reduction.

FTIR difference spectroscopy should provide an ideal tool for the analysis of the (micro)conformational changes associated with the redox transition. Indeed, the oxidized-minus-reduced difference spectra shown in Figures 4 and 5 exhibit sharp differential bands in the conformationally sensitive amide-I region (ca. 1600–1700 cm^{-1}), with amplitudes of a few milliabsorbance units compared to a total amide-I absorbance of approx. 0.5 AU. In this relation, we may interpret the sharp differential features as arising from individual peptide C=O groups—resumably of amino acids forming the Cu binding site—which respond to the new redox state. The possibility that multiple residues change their absorption only fractionally appears less likely, since, in this case, we would not expect very sharp, strong band structures because of initially heterogeneous absorbance bands.

Aside from peptide C=O groups exhibiting vibrational modes in this range according to the secondary structure in which they are involved, we have to consider the absorbance of amino acid side-chain residues [for a compilation of these frequencies, see Venyaminov and Kalnin (1990a)]. The NH_2^+ mode of His (around 1660 cm^{-1}), the C=O frequencies of Asn (abundant in halocyanin) and Gln (around 1680 and 1670, respectively), and the $CN_3H_5^+$ mode of Arg lead to distinct bands in this range, with molar extinction coefficients up to 500 L mol^{-1}cm^{-1} which are quite comparable to those of the peptide C=O modes [up to 700 L mol^{-1} cm^{-1}; *cf.* Venyaminov et al. (1990b)]. It should be noted, however, that the extinction coefficient for the His NH_2^+ is rather small (35 L mol^{-1} cm^{-1}), so that only minor contributions from these residues can be expected.

The effects of deuteration should allow us to distinguish between peptide C=O groups and side-chain modes in this range. Deuteration of Asn and Gln residues results in a downshift of the C=O mode from ca. 1680 to 1650 cm^{-1} (Asn) and from 1670 to 1635 cm^{-1} (Gln), while the $CN_3H_5^+$ mode of Arg shifts to approx. 1608 cm^{-1} (Venyaminov & Kalnin, 1990a; Chirgadze et al., 1975). None of the bands in Figure 4a, however, are found with either of these predicted shifts in the oxidized-minus-reduced difference spectrum of halocyanin in ^2H_2O. Instead, shifts of at most 3–4 cm^{-1} are detected, which are compatible with the properties of modes of peptide C=O bonds involved in a H-bonded structure.

In azurin, the peptide C=O group of Gly 45 has been proposed as a fifth ligand to the copper with a distance from the oxygen to the Cu of about 3 Å (Adman & Jensen, 1981). Similarly, plastocyanin has the peptide oxygen of Pro 36 at approx. 4 Å from the copper (Guss & Freeman, 1983). The oxidized-minus-reduced FTIR difference spectra of both azurin (M. Brischwein and W. Mäntele, unpublished data) and plastocyanin (Moss et al., 1989; M. Brischwein and W. Mäntele, unpublished data) exhibit a strong difference band at 1640–1650(+)/1625–1635(–) cm^{-1} analogous to that observed for halocyanin (Figure 4a). We thus assign this differential band structure to a peptide C=O group involved in coordinative binding to the Cu. Further support for this assignment comes from resonance Raman spectra of several azurins and of spinach plastocyanin (Siiman et al., 1974, 1976), which indicate resonance enhancement of an amide-I mode in the 1640–1660 cm^{-1} range.

The difference band shows a shift of the vibrational frequency to higher wavenumbers upon oxidation, which would be in agreement with an increase of the Cu–oxygen distance in the oxidized state (corresponding to a decrease of the C=O bond length). For a peptide C=O group, a distance increase of approx. 0.1 Å as proposed from X-ray crystallography would be sufficient to shift the C=O frequency significantly.

The second largest difference band at 1704(–)/1696(+) cm^{-1} is more difficult to assign. It is located at the high-frequency edge of the possible peptide C=O mode (Arrondo et al., 1993) and responds to ^1H–^2H substitution with only an approx. 2-cm^{-1} downshift. Since this band feature is conserved

in the FTIR difference spectra of plastocyanin, *Pseudomonas* azurin, and *Alcaligenes* azurin (M. Brischwein and W. Mäntele, unpublished observations), a conserved structural element or amino acid residue would present a potential candidate. Among the conserved residues, Asn 47 (in azurins) and Asn 38 (in plastocyanin) deserve special attention, since their peptide C=O oxygen is only about 5.6 Å from the copper (in *Alkaligenes* azurin). The corresponding residue in halocyanin could be Asn 31, Asn 57, or Gln 46, according to the amino acid sequence (S. Matter et al., unpublished data). In *Alcaligenes* azurin, this residue has been assigned a specific role in stabilizing the protein structure in the copper site (Guss & Freeman, 1983). Although the presumed H-bonding of this residue would tend to shift its frequency below 1680 cm^{-1}, we consider the peptide C=O group of this residue a potential candidate for the observed 1704/1696-cm^{-1} differential band.

If the redox transition were to alter the peptide C=O frequency of the Asn (or Gln) residue, one might also expect signals from the corresponding side-group C=O around 1680 cm^{-1} (^1H_2O) and 1650 cm^{-1} (^2H_2O). While the presumed peptide C=O frequency indicates a small isotope effect within the expected range, neither the sharp negative band at 1687 cm^{-1} nor the positive band at 1681 cm^{-1} shows the expected frequency shift. However, the intensity of the negative band at 1687 cm^{-1} is reduced considerably in ^2H_2O, which may be taken as a hint for the involvement of an Asn (Gln) residue.

In the 1600–1500 cm^{-1} range, two clear positive (1532 and 1572 cm^{-1}) and three negative peaks (1590, 1557, and 1516 cm^{-1}) are observed. While their absorption maxima are influenced only very little by ^1H–^2H substitution, there are changes of their relative intensities: the negative 1516 cm^{-1} peak is considerably weaker in ^2H_2O, as is the positive peak at 1572 cm^{-1}. Although one might think of an interpretation of these signals (at least the 1532- and 1557-cm^{-1} bands) in terms of amide-II modes, this seems unlikely, since the high degree of exchange of the peptide N-bound protons would lead to an almost complete disappearance of these bands. However, even in a small protein like halocyanin part of the protein structure could be inaccessible for deuteration. An alternative explanation for these difference bands could be signals from aromatic amino acid residues.

At alkaline pH, the oxidized-minus-reduced FTIR difference spectrum (Figure 5a) exhibits a negative band at 1535 cm^{-1}, which can still be seen at decreased amplitude at pH 8.6 (data not shown), but which has disappeared at pH 7 (Figure 4a). The negative band at 1652 cm^{-1} (i.e., the "dip" between the positive 1644 and 1663 cm^{-1} bands) decreases strongly toward high pH, a process which cannot merely be explained by the shifts of the positive bands (to 1661 and 1641 cm^{-1}, respectively).

The possible influence of histidines titrating at 3 (2) different pH values on the midpoint potential of azurin was discussed by Sykes (1991) and St. Clair et al. (1992). The pH dependence of the midpoint potential of halocyanin, which is quite comparable but exhibits a steeper slope, suggests that three residues titrate with pK values of 4.5, 6.5, and 8.3. In the pH-dependent oxidized-minus-reduced FTIR difference spectra, the protonation of histidine residues should be detectable by bands at around 1660 cm^{-1} (NH_2^+ deformation mode) which should appear/disappear as a function of pH. Furthermore, ^1H–^2H substitution should shift this putative His mode by approx. 30–40 cm^{-1} to lower wavenumbers. Although the negative band at 1652 cm^{-1} strongly decreases toward high pH, it cannot be interpreted along this line, since it is unaffected by ^1H–^2H substitution. In addition, its absorption appears too high for even several His side-chain residues, since the extinction coefficient for the NH_2^+ deformation mode is only about 35 L mol^{-1} cm^{-1} (Venyaminov & Kalnin, 1990a). In spite of the pH dependence of the redox midpoint potential, which would suggest, by analogy to azurins, titrating histidine residues, we presently cannot assign band structures in the IR difference spectra to vibrational modes of His side chains.

The most drastic effect in the oxidized-minus-reduced FTIR difference spectra occurs under acidic conditions (Figure 5b). Superimposed on a structured difference spectrum corresponding to that at neutral pH, except with small shifts of peak positions and changes of relative intensity, are a broad positive band between approx. 1750 and 1670 cm^{-1} and two negative bands centered at 1570 and 1400 cm^{-1}. The exact maximum of the positive band cannot be determined for reasons of overlap with the structured bands already discussed above in terms of peptide C=O groups. This feature starts to grow upon lowering of the pH to values below 6. It appears to reach its maximum amplitude when the pH is lowered toward 4; however, we were not able to titrate beyond this pH value since the complex became unstable and lost its blue color in the oxidized state.

In order to obtain approximate peak positions for this overlapping structure, we have subtracted an oxidized-minus-reduced difference spectrum obtained at pH 6 from one obtained under acidic conditions (Figure 5c). A weighted subtraction of the spectra of these two different samples yielded two broad negative bands at 1400 and 1570 cm^{-1} and a broad positive band at approx. 1700 cm^{-1}. Most of the structure in the negative bands at 1570 and 1400 cm^{-1} could be made to disappear by the choice of appropriate weighting factors; however, a residual fine structure remained in the broad positive band, indicating additional pH-dependent shifts of bands and changes of band intensities in the amide-I region between pH 6 and 4. It thus seems that the structural rearrangements at the copper-binding site are the same at low pH, but an additional process coupled to the redox reaction is observed.

The straightforward interpretation of the broad positive band at approx. 1700 cm^{-1} and the two broad negative bands at 1570 and 1400 cm^{-1} is the appearance of a carboxyl group C=O vibrational mode and the disappearance of the antisymmetric (1570 cm^{-1}) and the symmetric (1400 cm^{-1}) C—O mode of a carboxylate. Consequently, these coupled difference bands correspond to the protonation of an Asp or Glu side-chain residue upon oxidation of halocyanin. The intensity of the appearing and disappearing bands is in line with this interpretation, since both the COOH and the symmetric COO^- modes should have comparable extinction coefficients (200–300 L $mol^{-1}cm^{-1}$), and the antisymmetric COO^- mode should be somewhat stronger (350–450 L mol^{-1} cm^{-1}) (Venyaminov & Kalnin, 1990a). Although different half-widths could modify these extinction coefficients to some extent, we conclude by comparison of the amplitude of this band with the total amide-I band and the halocyanin concentration in the cell that oxidation of halocyanin under these condition results in protonation of one Asp or Glu residue. We further note that the half-widths of these bands are of the order of approx. 50 cm^{-1} as reported by Venyaminov and Kalnin (1990a) for aqueous solutions of amino acids. We may thus conclude that in halocyanin the respective side group is fully accessible to water and is not structurally constrained.

This oxidation-associated protonation in halocyanin, which has also been investigated in the *Pseudomonas* and *Alcaligenes*

azurins at about the same pH (M. Brischwein and W. Mäntele, unpublished observations) can be interpreted as an increase of the pK_a value of an Asp or Glu side-chain residue following oxidation of the Cu redox center, which leads to proton uptake at pH 5. Formally, this process can be written as

$$Cu^{+}\cdots R\text{–}COO^{-} + H^{+} \rightarrow Cu^{2+}\cdots R\text{–}COOH + e^{-}$$

The increase of the pK_a of this group could be caused by a (redox-induced) movement of the COO^- group with respect to a charge in the molecule. At present, we cannot decide whether the proton taken up originates from solution or from a donor group in the protein. A possible candidate for a C=O group with redox-dependent pK_a in azurins is the conserved residue Asp 11, located on the N-terminal loop approx. 9.5 (*Alcaligenes*) or 10.8 Å (*Pseudomonas*) away from the copper. As in the case of halocyanin, a closer attribution to specific residues has to await further studies with site-directed mutants.

An oxidation-induced proton uptake is contradictory with respect to the pH-dependent midpoint potential (*cf.* Figure 3). Proton uptake should result in a decrease of the midpoint potential with decreasing pH, in contrast to the further increase of E_m at low pH that is observed. At present, we can only explain this discrepancy by assuming that the effect of protonation of an Asp or Glu carboxylate group is compensated by deprotonation of one or two of the presumed His residues thought to interact with the redox center.

ACKNOWLEDGMENT

The authors would like to thank S. Grzybek for his help in developing software for instrument control and data treatment and to acknowledge excellent support by the workshops of the Institut für Biophysik, Freiburg (Mr. Merkt, Mr. Metzger, Mr. Sevenich, and co-workers). We thank Dr. M. Bauscher and F. Baymann for critical reading of the manuscript and Dr. Angelo di Bilio, California Institute of Technology, for samples of purified azurin.

REFERENCES

Adman, E. T. (1985) in *Topics in Molecular and Structural Biology: Metalloproteins* (Harrison, P., Ed.) Vol. I, pp 1–42, Macmillan, New York.

Adman, E. T., & Jensen, L. H. (1981) *Isr. J. Chem. 21*, 8–12.

Adman, E. T., Stenkamp, R. E., Sieker, L. C., & Jensen, L. H. (1978) *J. Mol. Biol. 123*, 35–47.

Ainscough, E. W., Bingham, A. G., Brodie, A. M., Ellis, W. R., Gray, H. B., Loehr, T. M., Plowman, J. E., Norris, G. E., & Baker, E. N. (1987) *Biochemistry 26*, 71–82.

Armstrong, E. A., Hill, H. A. O., Oliver, B. N., & Whitford, D. (1986) *Biochem. Soc. Trans. 14*, 283–316.

Arrondo, J. L. R., Muga, A., Castresana, J., & Goñi, F. M. (1993) *Prog. Biophys. Mol. Biol. 59*, 23–56.

Baymann, F., Moss, D. A., & Mäntele, W. (1991) *Anal. Biochemistry 199*, 269–274.

Brischwein, M. (1992) Master's Thesis, Department of Biology, Universität Freiburg.

Chirgadze, Y. N., Fedorov, O. V., & Trushina, N. P. (1975) *Biopolymers 14*, 679–694.

Colman, P. M., Freeman, H. C., Guss, J. M., Murata, M., Norris, V. A., Ramshaw, J. A. M., & Venkatappa, M. P. (1978) *Nature 272*, 319–324.

Dong, A., Huang, P., & Caughey, W. S. (1992) *Biochemistry 31*, 182–189.

Fritz, F., Moss, D. A., & Mäntele, W. (1991) *FEBS Lett. 297*, 167–170.

Groeneveld, C. M., Feiters, M. C., Hasnain, S. S., van Rijn, J., Reedijk, J., & Canters, G. W. (1986) *Biochim. Biophys. Acta 873*, 214–227.

Guss, J. M., & Freeman, H. C. (1983) *J. Mol. Biol. 169*, 521–563.

Hill, H. A. O., Page, D. J., Walton, N. J., & Whitford, D. (1985) *J. Electroanal. Chem. Interfacial Electrochem. 187*, 315–324.

Leonhard, M., & Mäntele, W. (1993) *Biochemistry 32*, 4532–4538.

Mäntele, W. (1993) in *The Photosynthetic Bacterial Reaction Center* (Deisenhofer, J., & Norris, J., Eds.) Vol. II, Chapter 10, pp 239–283, Academic Press, New York.

Mäntele, W., Leonhard, M., Bauscher, M., Nabedryk, E., Breton, J., & Moss, D. A. (1990) in *Reaction Centers of Photosynthetic Bacteria* (Michel-Beyerle, M. E., Ed.) Springer Series in Biophysics, Vol. 6, pp 31–44, Springer, Berlin.

Moss, D. A., Fritz, F., Haehnel, W., Breton, J., & Mäntele, W. (1989) in *Spectroscopy of Biological Molecules—State of the Art* (Bertoluzza, A., Fagnano, C., & Monti, P., Eds.) pp 355–356, Societa Editrice Aesculapia, Bologna, Italy.

Moss, D. A., Nabedryk, E., Breton, J., & Mäntele, W. (1990) *Eur. J. Biochem. 187*, 565–572.

Moss, D. A., Leonhard, M., Bauscher, M., & Mäntele, W. (1991) *FEBS Lett. 283*, 33–36.

Rydén, L. (1984) in *Copper Proteins and Copper Enzymes* (Lontie, R., Ed.) Vol. I, pp 157–182, CRC Press, Boca Raton, FL.

Scharf, B. (1992) Ph.D. Thesis, University of Bochum, Germany.

Scharf, B., & Engelhard, M. (1993) *Biochemistry* (in press).

Schlereth, D. D., & Mäntele, W. (1992) *Biochemistry 31*, 7494–7502.

Schlereth, D. D., & Mäntele, W. (1993) *Biochemistry 32*, 1118–1126.

Shepard, W., Anderson, B. F., Baker, E. N., & Norris, G. E. (1990) *Acta Crystallogr. C46*, 85.

Siiman, O., Young, N. M., & Paul, R. C. (1974) *J. Am. Chem. Soc. 96*, 5583–5585.

Siiman, O., Young, N. M., & Paul, R. C. (1976) *J. Am. Chem. Soc. 98*, 744–748.

St. Clair, C. S., Ellis, W. R., Jr., & Gray, H. B. (1992) *Inorg. Chim. Acta 191*, 149–155.

Sykes, A. G. (1985) *Chem. Soc. Rev. 14*, 283–316.

Sykes, A. G. (1991) in *Structure and Bonding* (Clark, M. J., et al., Eds.) Vol. 75, pp 175–224.

Takano, T., & Dickerson, R. E. (1981) *J. Mol. Biol. 153*, 95–115.

Venyaminov, S. Y., & Kalnin, N. N. (1990a) *Biopolymers 30*, 1243–1257.

Venyaminov, S. Y., & Kalnin, N. N. (1990b) *Biopolymers 30*, 1259–1271.